

Quantum-mechanical interference in two-photon absorption: A nonlinear analog of the Hanle effect

Gerald J. Diebold

Department of Chemistry, Brown University, Providence, Rhode Island 02912

(Received 26 October 1984; revised manuscript received 19 June 1985)

When an atom is irradiated by two light beams whose sum frequency corresponds to an allowed two-photon transition between two 1S states, no radiation is absorbed if the electric vectors of the two beams are perpendicular to each other. Application of a magnetic field in a direction perpendicular to the plane defined by the two electric vectors permits two-photon absorption to take place. According to quantum theory the effect is interpreted as an interference phenomenon. That is, if no field is applied, the intermediate states are degenerate and the interference is destructive; when a magnetic field is applied, two different paths through intermediate states are possible, permitting population of the upper state. The effect is related to the Hanle effect and likewise provides the basis for an experimental method of determining Landé factors.

I. INTRODUCTION

Although two-photon transitions have been studied theoretically¹ since the 1930s, it has only been with the introduction of the laser, with its characteristic high intensity and narrow bandwidth, that systematic experimental investigation of such nonlinear phenomena has been possible. According to quantum theory, the simultaneous absorption of two photons from two classical stable waves whose electric field amplitudes are small compared with the atomic Coulomb field is described by application of second-order perturbation theory. The salient features of two-photon absorption are a unique set of selection rules, a transition probability proportional to the product of the intensities of each wave (or to the square of the intensity of a single wave), and an enhancement in the absorption rate when the frequency of one of the waves is nearly coincident with an allowed single-photon transition.

This paper discusses an interference phenomenon that takes place in two-photon absorption. The effect is perhaps most clearly illustrated in an atomic 1S - 1S transition in which the frequency of one of the light beams is adjusted so as to be close to the frequency of a $^1P \leftarrow ^1S$ transition. In the expression for the transition probability to the upper 1S state the summation over intermediate or "virtual" states reduces to a sum over only the three magnetic sublevels of the 1P state. For two linearly polarized light beams that intersect with perpendicular electric vectors (see Fig. 1) destructive interference between the two beams takes place and the upper 1S state is not populated. The destructive interference is caused by the degeneracy of the $m = +1$ and -1 magnetic sublevels of the 1P intermediate state: because of the opposite phases of the two contributions to the transition probability there is an exact cancellation in the sum over the intermediate states giving a null overall excitation rate. If a magnetic field is applied in a direction perpendicular to the plane formed by the electric vectors of the two incident beams then the degeneracy of the magnetic sublevels of the 1P state is lifted giving two distinct paths for population of the excited

state. In this case the interference is only partially destructive and excitation to the upper state takes place at a rate proportional to the square of the magnetic field strength.

In Sec. II a classical theory of the effect is developed based on a nonlinear oscillator model of the atom. Sec-

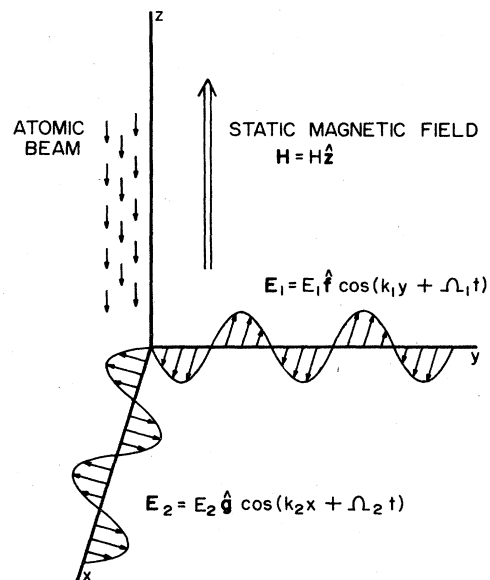


FIG. 1. Experimental arrangement for inducing two-photon transition free of the Doppler effect. Radiation with a wave vector \mathbf{k}_1 and frequency Ω_1 is directed along the Y axis. A second beam with wave vector \mathbf{k}_2 and frequency Ω_2 is directed along the X axis. In the classical calculation the unit vectors $\hat{\mathbf{f}}$ and $\hat{\mathbf{g}}$ that describe the polarization of the electric vectors are directed along the Y and X axes, respectively. In the quantum-mechanical calculation $\hat{\mathbf{f}}$ and $\hat{\mathbf{g}}$ are more general and are not restricted to the XY plane. An atomic beam is directed along the Z axis parallel to the magnetic field thus eliminating the first-order Doppler effect.

tion III gives a quantum-mechanical calculation of the interference using second-order perturbation theory. The results of the classical and quantum theories are found to be identical in the limit of large angular momentum. The interference effect is shown to provide an experimental method for determining Landé factors that depends only on measurement of a magnetic field strength and the detuning of a laser frequency from an atomic line.

II. CLASSICAL THEORY

The classical model used to explain the Zeeman effect² considers an atom to be comprised of a positive central charge with a harmonically attached electron subjected to a Lorentz force. The Lorentz force given by $(e/c)\mathbf{v}\times\mathbf{H}$, where \mathbf{v} is the velocity of the electron, e is its charge, \mathbf{H} is the magnetic field, and c is the speed of light, acts to rotate the direction of oscillation of the electron and at the same time alters the resonance frequency of the atom giving a "normal" Zeeman pattern. For the experimental arrangement shown in Fig. 1, the atom is irradiated by a light beam that is linearly polarized along the X axis, and whose angular frequency Ω_1 is approximately but not exactly equal to the resonance frequency of the atomic oscillator ω_0 . At the same time a second beam whose electric field polarization lies along the Y axis and whose angular frequency Ω_2 is far greater than ω_0 irradiates the atom.

It is clear that a model based on the harmonic oscillator is incapable of nonlinear effects such as two-photon absorption; thus the electron is assumed to move under the influence of both a harmonic potential and a potential of the form $(r-r_0)^3$, where r is the distance of the electron from the nucleus and r_0 is the rest distance of the electron from the nucleus. (The addition of a nonlinear force was originally used by Helmholtz³ to explain beat frequencies heard when musical tones of a slightly different pitch are played.) If E_1 and E_2 are the respective field amplitudes of the waves of frequencies Ω_1 and Ω_2 , then the equations of motion for the classical oscillator are

$$\frac{d^2x}{dt^2} + 2\gamma\frac{dx}{dt} + \omega_0^2x + \frac{F_x}{m} + 2M\frac{dy}{dt} = \frac{eE_1}{m}\cos(\Omega_1t), \quad (1a)$$

$$\frac{d^2y}{dt^2} + 2\gamma\frac{dy}{dt} + \omega_0^2y + \frac{F_y}{m} - 2M\frac{dx}{dt} = \frac{eE_2}{m}\cos(\Omega_2t), \quad (1b)$$

$$\frac{d^2z}{dt^2} + 2\gamma\frac{dz}{dt} + \omega_0^2z + \frac{F_z}{m} = 0, \quad (1c)$$

where x , y , and z are the displacements of the electron from equilibrium, m is the mass of the electron, M is defined according to

$$M = \frac{eH}{2mc}, \quad (2)$$

γ is a damping constant, and t is the time. F_x , F_y , and F_z are nonlinear forces which can be obtained for small amplitudes of vibration by a Taylor-series expansion of the potential about r_0 . When motion in the z direction is not excited, the terms F_x/m and F_y/m reduce to

$\epsilon(x^2 + 2xy + y^2)$, where ϵ is a constant of proportionality.

An exact solution to such coupled nonlinear differential equations is not apparent; however, if the nonlinear term is small then perturbative methods of solution can be applied. As outlined in the Appendix, the method of reversion⁴ used for solution of nonlinear differential equations in one variable can be extended to coupled nonlinear equations. The procedure consists of first solving the coupled equations ignoring the nonlinear terms. Then, this approximate solution is substituted into the nonlinear terms which are then considered as forcing functions. For the purposes of this calculation an approximate solution that is a superposition of the linear solution and the lowest-order correction due to the nonlinear terms is used.

Solution to the coupled linear equations can be obtained by linear superposition of the motions resulting from each electric field considered separately. Provided Ω_2 is far enough from resonance so that $|\omega_0 - \Omega_2| \gg 2\gamma$ and $|\omega_0 - \Omega_2| \gg 2M$, and given the assumption that Ω_1 is close to resonance so $\omega_0^2 - \Omega_1^2 \cong 2\omega_0\Delta$, where

$$\Delta = \omega_0 - \Omega_1, \quad (3)$$

then the solution of Eqs. (1a) and (1b) to lowest order is given by

$$x_1 = \frac{eE_1}{2m\omega_0} \frac{(\Delta^2 + \gamma^2)^{1/2} \cos(\Omega_1t - \phi_x)}{[(\Delta^2 - \gamma^2 - M^2)^2 + 4\gamma^2\Delta^2]^{1/2}} + \frac{2eE_2}{m} \frac{\Omega_2 M \sin(\Omega_2t)}{(\omega_0^2 - \Omega_2^2)^2}, \quad (4a)$$

$$y_1 = \frac{eE_2}{m} \frac{\cos(\Omega_2t)}{\omega_0^2 - \Omega_2^2} - \frac{eE_1}{2m\omega_0} \frac{M \sin(\Omega_1t - \phi_y)}{[(\Delta^2 - \gamma^2 - M^2)^2 + 4\gamma^2\Delta^2]^{1/2}}, \quad (4b)$$

where

$$\phi_x = \tan^{-1} \left[\frac{\gamma(\Delta^2 + \gamma^2 + M^2)}{\Delta(\Delta^2 + \gamma^2 - M^2)} \right],$$

$$\phi_y = \tan^{-1} \left[\frac{2\gamma\Delta}{\Delta^2 - \gamma^2 - M^2} \right].$$

It is easy to see that the field E_1 induces a dipole moment varying with time along the X direction which is swept into the Y direction by the magnetic field. The same process is caused by application of the field E_2 , but as its frequency is far from resonance the magnitude of the induced polarization is much smaller. When the magnetic field is zero, a large displacement of the electron in the X direction but only a small displacement in the Y direction is produced. The motions of the electron along the X and Y directions in zero field are independent only in the first-order approximation since the nonlinear force causes coupling between the x and y equations.

Two-photon absorption arises from mixing of the first-order sinusoidal solutions by the nonlinear force terms in Eqs. (1). If the leading terms in the forcing function at a frequency $\Omega_1 + \Omega_2$ are collected, the correction to the first-order solution, according to the Appendix, is the solution to the equations

$$\left. \begin{aligned} \frac{d^2x}{dt^2} + 2\gamma \frac{dx}{dt} + \omega_0^2 x + 2M \frac{dy}{dt} \\ \frac{d^2y}{dt^2} + 2\gamma \frac{dy}{dt} + \omega_0^2 y - 2M \frac{dx}{dt} \end{aligned} \right\} = -\epsilon \frac{\frac{eE_1}{2\omega_0} \frac{eE_2}{m}}{[(\Delta^2 - \gamma^2 - M^2)^2 + 4\gamma^2 \Delta^2]^{1/2} (\omega_0^2 - \Omega_2^2)} \times \{(\Delta^2 + \gamma^2)^{1/2} \cos[(\Omega_1 + \Omega_2)t - \phi_x] - M \sin[(\Omega_1 + \Omega_2)t - \phi_y]\}. \quad (5)$$

The solution to these equations gives the electronic coordinates, from which the velocity can be found. The power absorbed at the sum frequency $\Omega_1 + \Omega_2$ by the oscillating electron $P_{\Omega_1 + \Omega_2}$ is given by the time average of the product of the damping force and the velocity,

$$P_{\Omega_1 + \Omega_2} = \left\langle 2m\gamma \left[\frac{dy_2}{dt} \right]^2 + 2m\gamma \left[\frac{dx_2}{dt} \right]^2 \right\rangle \quad (6)$$

which becomes

$$P_{\Omega_1 + \Omega_2} = I_1 I_2 \frac{\Delta^2 + M^2 + \gamma^2}{[(\Delta + M)^2 + \gamma^2][(\Delta - M)^2 + \gamma^2]}, \quad (7)$$

where I_1 and I_2 are the intensities of the two beams, proportional to the squares of E_1 and E_2 , respectively. [Unimportant factors independent of M have been deleted from Eq. (7).]

The nonlinear force term of the form ϵxy is responsible for two-photon absorption in Eq. (7) proportional to $\Delta^2 + \gamma^2$. The remaining term in $P_{\Omega_1 + \Omega_2}$ proportional to M^2 arises from rotation of the induced dipole created by E_1 into the Y direction which permits interaction between the two fields (via the ϵy^2 force term) to produce two-photon absorption. Equation (7) predicts, as expected, an absorption proportional to the product of the intensities of the two beams. In addition, $P_{\Omega_1 + \Omega_2}$ is symmetrical with respect to a reflection of H in the XY plane (i.e., $M \rightarrow -M$). This follows from the classical model of the Zeeman effect where the presence of a magnetic field gives solutions to the equations of motion that describe both clockwise and counterclockwise rotation of the electron about the field direction—reversal of the direction of H gives the same clockwise and counterclockwise motions of the electron.

III. QUANTUM THEORY

A number of reviews treating several aspects of multi-photon absorption exist.⁵⁻¹⁰ To some extent the results presented here are implicit in the formulas previously obtained by other authors.¹¹ However, for the conditions of an experiment envisioned here an important simplification of the usual transition rate expression obtains; in addition, particular focus must be given to polarization effects and the influence of a static external field. For these reasons, a brief perturbation calculation¹² of the two-photon transition rate is given.

According to perturbation theory, the state of an atom is described by a wave function Ψ that can be expanded in terms of the energy eigenstates Ψ_i as

$$\Psi = \sum_n b_n(t) \Psi_n e^{-iE_n t/\hbar}, \quad (8)$$

where $|b_i(t)|^2$ is the probability that the atom is in the state i and E_i is the energy of the state i . For a time-dependent perturbation $V(t)$ the probability amplitudes $b_i(t)$ vary in time as described by the Schrödinger equation which can be written

$$i\hbar \frac{db_m(t)}{dt} = \sum_n V_{mn}(t) b_n(t) e^{i\omega_{mn}t}, \quad (9)$$

where $V_{mn}(t) = \langle m | V(t) | n \rangle$, and ω_{mn} is the difference in the energies of the states m and n divided by \hbar (Planck's constant divided by 2π).

Consider a light beam with an electric field polarization \hat{f} at a frequency Ω_1 that is adjusted to be nearly coincident with the energy-level splitting between a 1P and a 1S state (i.e., in the notation of Fig. 2, $\hbar\omega_1 \cong E_\mu - E_m$). Also, let the atom be irradiated by a second beam with polarization \hat{g} , at a frequency Ω_2 that differs greatly from the 1P ground-state splitting, but that is adjusted to be of such frequency that together with the first beam two photons can be absorbed to excite an upper 1S state, that is, $\hbar(\Omega_1 + \Omega_2) = E_\eta - E_m$. According to Eq. (9) the equations of motion for the probability amplitude $b_\mu(t)$ include contributions from perturbations by both radiation beams; however, provided Ω_1 is nearly resonant with the states μ , and Ω_2 is far from resonance, the contribution of the first beam is dominant and the probability amplitude $b_\eta(t)$ for the excited 1S state η can be shown to be

$$b_\eta(t) = \sum_\mu \frac{H_{\eta\mu}^{g*} H_{\mu m}^f}{\hbar^2} \times \frac{e^{i[\omega_{\eta m} - (\Omega_1 + \Omega_2)]t} - 1}{[(\omega_\mu - \Omega_1) - i\Gamma/2][\omega_{\eta m} - (\Omega_1 + \Omega_2)]}, \quad (10)$$

where Γ is a damping constant describing spontaneous emission, where the frequencies ω_μ and $\omega_{\eta m}$ are defined as $\omega_\mu = (E_\mu - E_m)/\hbar$ and $\omega_{\eta m} = (E_\eta - E_m)/\hbar$, and where the electric dipole matrix elements $H_{\mu m}^f$ and $H_{\eta\mu}^g$ are given by

$$H_{\mu m}^f = eE_1 \langle ^1P, \mu | \hat{f} \cdot \mathbf{r} | ^1S, m \rangle,$$

$$H_{\eta\mu}^g = eE_2 \langle ^1P, \mu | \hat{g} \cdot \mathbf{r} | ^1S, \eta \rangle.$$

The rate of population of the state η , denoted R , is the probability per unit time of finding the atom in the state η , so that $R = |b_\eta(t)|^2/t$. The expression for R is simplified using the relation

$$\lim_{t \rightarrow \infty} \left| \frac{e^{i[\omega_{\eta m} - (\Omega_1 + \Omega_2)]t} - 1}{\omega_{\eta m} - (\Omega_1 + \Omega_2)} \right|^2 = \pi t \delta(\omega_{\eta m} - (\Omega_1 + \Omega_2)), \quad (11)$$

where $\delta(\omega_{\eta m} - (\Omega_1 + \Omega_2))$ is the Dirac delta function. The rate of population of the upper 1S state can then be written

$$R = \pi \sum_{\mu, \mu'} \frac{F_{\mu\mu'} G_{\mu'\mu}}{[(\omega_{\mu} - \Omega_1) - i\Gamma/2][(\omega_{\mu'} - \Omega_1) + i\Gamma/2]} \times \delta(\omega_{\eta m} - (\Omega_1 + \Omega_2)), \quad (12)$$

where the matrices F and G are defined by

$$F_{\mu\mu'} = H_{\mu m}^f H_{m\mu'}^f \quad \text{and} \quad G_{\mu'\mu} = H_{\mu'\eta}^g H_{\eta\mu}^g.$$

This describes the essential features of the two-photon interference for any perturbation that alters the spacing of the intermediate levels. To be more explicit both the matrix elements and the field dependence of the intermediate states must be specified.

The matrix elements in Eq. (18) are found by first writing $\hat{\mathbf{f}} \cdot \mathbf{r}$ in tensor form,

$$\hat{\mathbf{f}} \cdot \mathbf{r} = \sum_q (-1)^q f_q r_{-q}, \quad (13)$$

where $f_{\pm 1} = \mp(f_x \pm if_y)/\sqrt{2}$ and $f_0 = f_z$ (the spherical components r_q are defined similarly). The Wigner-Eckart theorem¹³ can then be used to give

$$H_{\pm 10}^f = -eE_1 \langle 1 || r || 0 \rangle f_{\mp 1} \quad (14)$$

and

$$H_{00}^f = eE_1 \langle 1 || r || 0 \rangle f_0,$$

where the factors multiplying the unit vectors are the usual reduced matrix elements. From this result the matrix F can be constructed giving

$$F = \begin{matrix} & -1 & 0 & +1 \\ -1 & \left[\begin{array}{ccc} -f_{-1}f_{+1} & -f_0f_{+1} & -f_{+1}^2 \\ f_{-1}f_0 & f_0 & f_0f_{+1} \\ -f_{-1}^2 & -f_{-1}f_0 & -f_{-1}f_{+1} \end{array} \right] & & \\ 0 & & & & \\ +1 & & & & \end{matrix} |\langle 1 || r || 0 \rangle|^2 (eE_1)^2. \quad (15)$$

It is easy to show, for the problem at hand, that the G matrix is the same as the F matrix but with $g_{\pm 1}$ substituted for $f_{\pm 1}$ and g_0 substituted for f_0 . The reduced matrix element must also be changed to correspond to the $^1S \leftarrow ^1P$ transition, and, of course, E_2 must be substituted for E_1 . Note that the polarization vectors $\hat{\mathbf{f}}$ and $\hat{\mathbf{g}}$ can be described in terms of three angles as shown in Fig. 3. The components of $\hat{\mathbf{f}}$ in a spherical basis are given by¹⁴

$$f_{\pm 1} = \frac{\mp 1}{\sqrt{2}} (\cos\theta_f \cos\alpha_f \pm i \sin\alpha_f) e^{\pm i\phi_f}, \quad (16)$$

$$f_0 = -\sin\theta_f \cos\alpha_f.$$

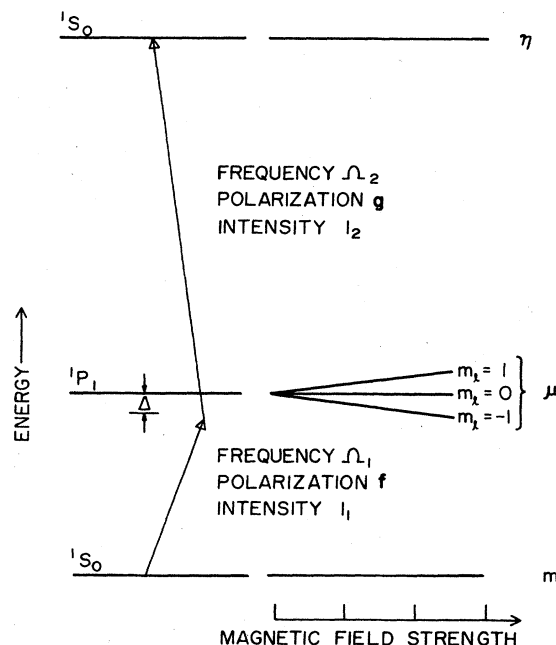


FIG. 2. Energy-level diagram for an atom in which a $^1S \leftarrow ^1S$ transition is induced by absorption of two photons. In the classical model the splitting between the ground state and the 1P state corresponds to ω_0 , the resonance frequency of the oscillator. Application of a magnetic field causes a splitting of the energy levels of the 1P state into three levels, ω_0 and $\omega_0 \pm M$. In the quantum-mechanical calculation, the magnetic field removes the degeneracy of the three magnetic sublevels $m_l = 0, \pm 1$ (denoted by μ); the energy splittings are identical with those calculated by classical theory. The radiation beam with a frequency Ω_1 and polarization $\hat{\mathbf{f}}$ is adjusted so that Ω_1 is nearly, but not exactly equal to the 1P ground-state energy splitting. The radiation with polarization $\hat{\mathbf{g}}$ has a frequency Ω_2 that is far from the 1P ground-state energy splitting.

The components of $\hat{\mathbf{g}}$ in a spherical basis are defined similarly with subscripts g instead of f .

It is convenient to group the various contributions to R according to values of $\Delta\mu$ which range from 0 to 2. If the summation in Eq. (12) is carried out over the appropriate values of μ and μ' and the matrix elements of F and G are substituted into the resulting expression, then R can be written as a sum of three terms,

$$R = R(\Delta\mu = 0) + R(\Delta\mu = 1) + R(\Delta\mu = 2). \quad (17)$$

The term $R(\Delta\mu = 2)$, for instance, is given by

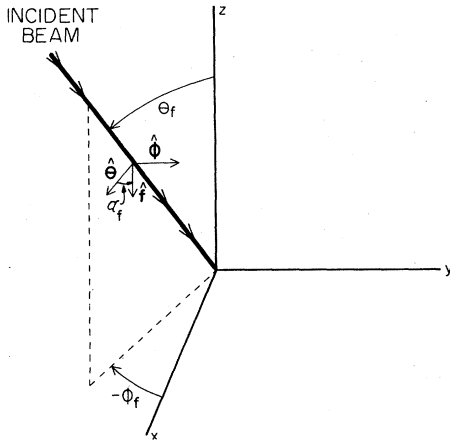


FIG. 3. Description of the angles θ_f , ϕ_f , and α_f that determine the direction of the incident linearly polarized radiation. The angles θ_f and ϕ_f are the ordinary azimuthal and polar angles used in spherical coordinates; α_f is measured from the unit vector $\hat{\theta}$ and describes rotation of the polarization vector \hat{p} about the propagation vector \mathbf{k}_1 . An identical system is used to describe the orientation of \hat{g} in terms of θ_g , ϕ_g , and α_g .

$$R(\Delta\mu=2) = \frac{f_{+1}^2 g_{-1}^2}{[(\omega_{-1} - \Omega_1) - i\Gamma/2][(\omega_{+1} - \Omega_1) + i\Gamma/2]} + \frac{f_{-1}^2 g_{+1}^2}{[(\omega_{+1} - \Omega_1) - i\Gamma/2][(\omega_{-1} - \Omega_1) + i\Gamma/2]}$$

other terms are found similarly by substitution of the elements of F and G into Eq. (12).

The description of the incident beam geometry thus far has been general; at this point the beam directions and polarizations can be specified and the excitation rate calculated. If the configuration in Fig. 1 is used where the two beams intersect at right angles with \hat{f} and \hat{g} in the XY plane, then Eqs. (16) reduce to $f_{\pm 1} = \mp 1/\sqrt{2}$, $f_0 = 0$, $g_{\pm 1} = \mp i/\sqrt{2}$, and $g_0 = 0$. Furthermore, the resonance frequency of the atom in the laboratory reference frame remains unchanged since there is no first-order Doppler effect; thus, the following substitutions can be made in evaluating Eq. (17):

$$\omega_{\pm 1} - \Omega_1 = \Delta \pm g\beta H/\hbar, \quad (18)$$

where the detuning of Ω_1 from resonance Δ is defined as in Eq. (3), where the Bohr magneton β is given by $\beta = \hbar/2mc$, and where g is the Landé factor for the intermediate state. (In the absence of perturbations, g equals 1 for a 1P state.) With these substitutions Eq. (17) reduces to a sum of terms over $\Delta\mu = 0$ and 2 giving an excitation rate

$$R = \frac{I_1 I_2 (g\beta H/\hbar)^2}{[(\Delta + g\beta H/\hbar)^2 + \Gamma^2/4][(\Delta - g\beta H/\hbar)^2 + \Gamma^2/4]}, \quad (19)$$

where unimportant numerical constants have been factored out of the final result.

In the limit of large angular momentum, the quantum-mechanical two-photon absorption rate is expected to ap-

proach the classical result obtained in Sec. II. To calculate the former, the expression for R in Eq. (12) must be generalized to include a sum over magnetic sublevels of the ground state. It is easy to see for a transition of the form $^1(L+2) \leftarrow ^1(L+1) \leftarrow ^1L$, that for a given magnetic sublevel of the ground state m , there are four pathways for excitation of the $^1(L+2)$ level when the polarization specified in Fig. 1 is used. Two of the pathways are transitions between sublevels with the same magnetic quantum numbers (i.e., $\eta = m$); these two pathways interfere giving a contribution $R_{m,m}$ to the overall rate that is proportional to the right-hand side of Eq. (19). The two other pathways correspond to transitions to the states $\eta = m+2$ and $\eta = m-2$, the rates for which are denoted $R_{m+2,m}$ and $R_{m-2,m}$, respectively. The overall rate of population of the upper state R is an incoherent sum of the interfering and noninterfering rates over all the magnetic sublevels of the ground state, or $R = \sum_m (R_{m,m} + R_{m+2,m} + R_{m-2,m})$. Now, if the noninterfering terms are grouped in pairs with opposite signs for m , then each pair gives a contribution to R proportional to the right-hand side of Eq. (19), but with $(g\beta H/\hbar)^2$ in the numerator replaced by $\Delta^2 + (g\beta H/\hbar)^2 + \Gamma^2/4$. It is not difficult to show that for $\mu > 0$, when $\mu = m+1$ the numerical factor in the ratio $R_{m+2}/R_{m,m}$ is

$$(L + \mu + 2)(L + \mu + 4)/(L - \mu + 2)(L - \mu + 3),$$

a quantity that is greater than 1. As μ approaches $L+1$, this ratio becomes $2L^2$, which becomes arbitrarily large for large L . Thus, the noninterfering pathways for population of the upper state become dominant and the quantum-mechanical absorption rate approaches the classical expression given by Eq. (7) insofar as the field dependence is concerned. Note that the Landé factor for any singlet state is always 1, and that 2γ in the classical picture corresponds to Γ in the quantum theory as can be seen by equating power dissipation rates.

Since the majority of multiphoton excitation experiments are carried out with either a single beam, or with beams having parallel polarizations, it is of some interest to determine the sensitivity of the excitation rate to the presence of magnetic fields. This is conveniently done by considering the same geometry as in Fig. 1, but with the two beams collinear and with the polarization vectors in the XY plane. The result of a calculation for a $^1S \leftarrow ^1S$ transition shows R to be identical with the expression obtained in Eq. (19) but with the numerator replaced by $I_1 I_2 (\Delta^2 + \Gamma^2/4)$. Thus, only in the event that one of the beams is tuned close to an atomic resonance frequency will a magnetic field be of importance.

IV. DETERMINATION OF LANDÉ FACTORS

The dependence of the two-photon excitation rate on the detuning and magnetic field given in Eq. (19) suggests that experimental measurements of the excitation rate as a function of magnetic field might provide a method for determining Landé factors. The direct dependence of R on g and H in the numerator at first sight appears to provide a straightforward method of determining the g fac-

tor; in fact, an absolute measurement of R is required in order to determine g . This clearly is impractical.

For experimental determination of Landé factors consider the following geometrical arrangement of incident radiation polarization vectors as shown in Fig. 4. Let both \mathbf{k}_1 and \mathbf{k}_2 be directed along the Z axis (so they are either parallel or antiparallel—the result depends on the orientation of the polarization vectors, not on the propa-

gation vectors). Place the polarization vector of E_1 (i.e., $\hat{\mathbf{f}}$) along the X axis and let E_2 (i.e., $\hat{\mathbf{g}}$) be rotated by a polarization rotation device such as a half-wave Fresnel rhomb. The molecular beam is directed along the X axis and the magnetic field is again placed along the Z axis. This arrangement again provides Doppler-free excitation as the radiation beams propagate perpendicularly to the atomic beam. Equation (17) can be evaluated to give

$$R = I_1 I_2 \frac{\cos^2 \phi_g \left[\frac{g\beta H}{\hbar} \right]^2 + \sin^2 \phi_g (\Delta^2 + \Gamma^2/4) + \cos \phi_g \sin \phi_g \left[\frac{g\beta H \Gamma}{\hbar} \right]}{[(\Delta + g\beta H/\hbar)^2 + \Gamma^2/4][(\Delta - g\beta H/\hbar)^2 + \Gamma^2/4]} \quad (20)$$

When $\phi_g = 0$, the electric vectors of the two beams are perpendicular and the numerator of Eq. (20) becomes $I_1 I_2 (g\beta H/\hbar)^2$. As ϕ_g is rotated to $\pi/2$ the numerator becomes $I_1 I_2 (\Delta^2 + \Gamma^2/4)$. Two important experimental advantages for measurement of g factors are obtained using this approach. First, the measurement of R is now referenced to Δ instead of being an absolute measurement. Second, the Landé factor is determined directly from a knowledge of Δ , H , and the measured excitation rate. (It has been assumed that Δ is adjusted in any experiment to make $\Gamma/2|\Delta| \ll 1$.)

Consider an experiment with an atomic beam of Ca. In general, if $\Delta \gg \mathbf{k} \cdot \mathbf{v}$ where \mathbf{v} is the beam velocity, then any residual Doppler effect can be ignored. The $^1P \leftarrow ^1S$ transition in Ca is excited by 422.7-nm radiation while the $4p^2^1S \leftarrow ^1P$ transition is excited by 586.8-nm radiation. For the 1P state, Γ is $2.18 \times 10^8 \text{ s}^{-1}$. If $\Delta/2\pi$ is adjusted to be 2.8 GHz then $(\Gamma/2\Delta)^2$ is 3.8×10^{-5} so that the error from neglecting Γ can be ignored. (That is, the precision in the measurement of H or the signal-to-noise ratio in

the data will, in all certainty, be greater than this.) For a g factor of unity (and with $\beta/\hbar = 1.3997 \text{ MHz/G}$) the magnetic-field-induced excitation rate at a field of 1 kG will be 25% of the rate with the two electric fields in the parallel configuration. Thus the two excitation rates should be comparable giving not too disparate signal-to-noise ratios in the detected signals.

A limitation to the accuracy of Landé-factor determinations by the above method comes from energy-level shifts due to the ac Stark effect. According to Jaynes and Cummings,¹⁵ or Stroud¹⁶ (see also Refs. 7 and 17 for reviews), the ac Stark effect shifts energy levels of the 1P levels in the low-intensity limit by an amount¹⁸

$$\Delta E_\mu = \frac{e^2 E_1^2}{2\hbar} \frac{|H_{\mu m}^f|^2}{\Delta} \quad (21)$$

Here, it is assumed that since the detuning of Ω_1 from resonance is so much smaller than the corresponding detuning of Ω_2 from the 1P ground-state energy-level splitting that the former dominates the Stark shift. (If E_2 is inordinately large for some reason then its effect must also be included despite its assumed large detuning.) The energy shift corresponding to the Block-Siegert shift in the expression for ΔE_μ has also been deleted since it is small at optical frequencies. The same calculation shows that the shift in the energy level of the ground state is of the same order of magnitude but of the opposite sign; that is, with Δ positive the levels μ are shifted to higher energy while the ground state is shifted to lower energy.

Experimental measurements of the ac Stark effect have been made by Liao and Bjorkholm¹⁹ and by Bonch-Bruевич, Kostin, Khodovoi, and Khomov.²⁰ Liao and Bjorkholm find a linear increase in the energy shift with radiation intensity (i.e., as E_1^2) at a rate of 300 MHz/(kW/cm²) with a detuning of 4 GHz for a strongly allowed transition in atomic Na. The authors note that it is possible to eliminate the ac Stark effect altogether by appropriate attenuation of the radiation beam while still maintaining enough power density to observe fluorescence from the excited state. It is evident that if high intensity is required to observe the two-photon population rate (by whatever mechanism it is monitored) then from the perspective of reducing the Stark effect it is prudent to in-

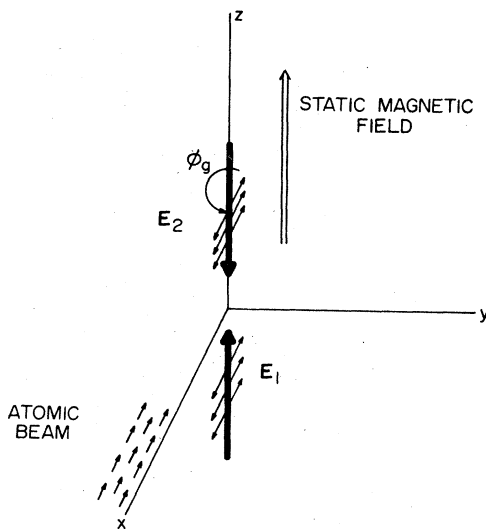


FIG. 4. Doppler-free geometry for carrying out experimental measurements of Landé factors.

crease I_2 , which is far from resonance, rather than I_1 since the population rate depends on the product of both I_1 and I_2 whereas the ac Stark effect is dominated only by the beam with intensity I_1 .

Determination of Landé factors by this method is seen to depend upon a measurement of the detuning, the magnetic field, and the rate of population of the excited state. Using devices, such as an optical wavemeter, the detuning can be determined precisely; magnetic fields can also be measured with high accuracy using nuclear magnetic resonance techniques. The overall accuracy of such a Landé-factor measurement depends on such factors as the signal-to-noise ratio in the recorded signal, which is increased, as discussed above, at the expense of possible ac Stark shifts. It would appear then that determination of the overall accuracy of a Landé-factor measurement would be more appropriately addressed by reference to actual experimental data than to further calculations.

V. DISCUSSION

Comparison of the two-photon interference effect described here with the Hanle effect²¹⁻²⁵ shows both similarities and differences that serve to delineate several features of these effects. Both phenomena are quantum-mechanical interference effects that depend on the existence of two paths for population of the final state. For the two-photon absorption discussed here the linearly polarized light with polarization along with Y axis can be resolved into right- and left-hand circularly polarized components (σ^- and σ^+ radiation) that create a polarization varying with time at a frequency Ω_1 in the $m_l = +1$ and -1 sublevels of the 1P state. The second beam at a frequency Ω_2 also can be resolved into σ^- and σ^+ components that interact with the polarization produced by the first beam to populate the excited state. There are two routes to excitation of the upper state: absorption of a σ^+ photon at a frequency Ω_1 followed by absorption of a second σ^- photon at a frequency Ω_2 , or alternately, absorption of a σ^- photon from the first beam followed by absorption of a σ^+ photon from the second beam. In a Hanle effect experiment on a $^1P-^1S$ transition where fluorescence is detected at right angles to an exciting beam the same paths exist, but the absorption of the second photon is replaced by emission of a fluorescence photon. In both cases the interference phenomenon is contingent on the existence of two paths to the final state. Not to be overlooked is the fact that the vector \hat{f} must be placed so that the polarization of the intermediate state, or in the case of Hanle effect, the populations of the $m_l = \pm 1$ states, is prepared in a coherent superposition.²⁶ Not only must there be two paths leading to the final state but also a definite phase relation between the paths must exist. In fact, this is guaranteed in both the Hanle effect and the two-photon effect described here by placement of the electric vector of the incident beam (E_1 in this paper) perpendicular to the quantization axis defined by the magnetic field. (If, for instance, \hat{f} and \hat{g} are placed along the z axis no interference takes place.)

An important contrast between the two-photon interference and the Hanle interference is that only the latter is a

Doppler-free effect. As is well known, the exciting radiation in a Hanle-effect experiment should be of a sufficiently wide bandwidth to excite the magnetic sublevels of the excited state independently of their field splittings. As the radiation bandwidth is broad there is no effect caused by the motional broadening from the Doppler effect. This can be seen in the Hanle-effect formulas for the scattered radiation intensity where ω_0 does not appear explicitly. For the two-photon interference, Eq. (19) shows that R depends on ω_0 and Ω_1 through Δ and hence any shift in Δ from the Doppler effect acts to change the magnitude of R . However, since atomic beams are produced perhaps with greater ease than are static entrapments of atoms in buffer gases, the restriction on the observation of this effect to Doppler-free geometrical arrangements does not appear to be excessively severe.

An enlightening contrast between the Hanle and two-photon interference effects can be found in their classical derivations. The Hanle effect, which can be described as a rotation of the dipole radiation pattern by the Lorentz force on the oscillating electron, is derived from the transient solution to the *homogeneous* equations of motion for the electron given by Eqs. (1) (with $\epsilon=0$). The two-photon absorption, on the other hand, relies wholly on the steady-state, *inhomogeneous* solution to the electronic equations of motion. The nonlinearity essential to the equations of motion for two-photon interference is of course another important distinction between the mechanisms for the two effect.

Although the interference effect is discussed here with emphasis on a two-photon excitation of a 1S state from a 1S ground state through a 1P intermediate state, it is not difficult to derive a result similar to Eq. (19) in more complicated cases involving states with higher angular momentum or hyperfine coupling following the same procedure given in Sec. III. Moreover, since the two-photon interference described here is of the nature of a zero-field level-crossing effect, the extension of the interference to high-field crossings appears to be straightforward.

ACKNOWLEDGMENT

The author is grateful for the partial support of this research by the Office of Basic Energy Studies of the U.S. Department of Energy.

APPENDIX

Equations (1a) and (1b) are of the form

$$a \begin{bmatrix} x \\ y \end{bmatrix} + \epsilon \begin{bmatrix} (x+y)^2 \\ (x+y)^2 \end{bmatrix} = \kappa \begin{bmatrix} 1 & 0 \\ 0 & 1 \end{bmatrix} \begin{bmatrix} \phi_1(t) \\ \phi_2(t) \end{bmatrix}, \quad (\text{A1})$$

where ϕ_1 and ϕ_2 are driving functions, the matrix a is a linear operator given by

$$a = \begin{bmatrix} D^2 + 2\gamma D + \omega_0^2 & + 2MD \\ + 2MD & D^2 + 2\gamma D + \omega_0^2 \end{bmatrix}, \quad (\text{A2})$$

where $D = d/dt$, and κ is a constant. A perturbation solution to Eq. (A1) can be developed in analogy with the method of reversion given by Pipes⁴ by considering a power-series expansion of the solution of the form

$$\begin{bmatrix} x \\ y \end{bmatrix} = \begin{bmatrix} x_1 \\ y_1 \end{bmatrix} \kappa + \begin{bmatrix} x_2 \\ y_2 \end{bmatrix} \kappa^2 + \begin{bmatrix} x_3 \\ y_3 \end{bmatrix} \kappa^3 + \dots \quad (\text{A3})$$

If this expansion is substituted into Eq. (A1) and coefficients with equal powers of κ are equated then a series of linear differential equations results, the two lowest-order differential equations in which are given by

$$\begin{bmatrix} a \\ a \end{bmatrix} \begin{bmatrix} x_1 \\ y_1 \end{bmatrix} = \begin{bmatrix} \phi_1(t) \\ \phi_2(t) \end{bmatrix} \quad (\text{A4})$$

and

$$\begin{bmatrix} a \\ a \end{bmatrix} \begin{bmatrix} x_2 \\ y_2 \end{bmatrix} = -\epsilon \begin{bmatrix} x_1^2 + 2x_1y_1 + y_1^2 \\ x_1^2 + 2x_1y_1 + y_1^2 \end{bmatrix}. \quad (\text{A5})$$

The procedure requires a solution to the linear equations (A4) giving x_1 and y_1 ; the solution to (A4) is substituted into Eq. (A5) to give a second linear differential equation whose solution is a correction to (x_1, y_1) .

¹M. Goppert-Mayer, *Ann. Phys. (Leipzig)* **9**, 273 (1931).

²P. P. Feofilov, *The Physical Basis of Polarized Light* (Consultants Bureau, New York, 1961).

³H. Helmholtz, *Sensations of Tone* (Longmans, Green, London, 1885).

⁴L. A. Pipes, *Operational Methods in Nonlinear Mechanics* (Dover, New York, 1965).

⁵P. Lambropoulos, in *Advances in Atomic and Molecular Physics*, edited by D. R. Bates and B. Bederson (Academic, New York, 1976), Vol. 12.

⁶F. Giacobino and B. Cagnac, in *Progress in Optics*, edited by E. Wolf (North-Holland, New York, 1980).

⁷J. S. Bakos, *Phys. Reports*, **31**, 209 (1977).

⁸*Multiphoton Processes*, edited by J. H. Eberly and P. Lambropoulos (Wiley, New York, 1978).

⁹A. Schenzle and R. G. Brewer, *Phys. Rep.* **43**, 455 (1978).

¹⁰L. Allen and C. R. Stroud, Jr., *Phys. Rep.* **91**, 2 (1982).

¹¹Effects due to orientation of polarization vectors of the radiation have been discussed by G. Grynberg, F. Beraben, E. Giacobino, and B. Cagnac in *J. Phys. (Paris)* **38**, 629 (1977); *Opt. Commun.* **18**, 374 (1976); however, the only interference effects mentioned are found in the absence of an external field.

¹²The calculation given here follows W. Heitler, *The Quantum Theory of Radiation*, 3rd. ed. (Oxford University, London, 1954), Chap. IV. See also J. L. Powell and B. Craseman, *Quantum Mechanics* (Addison-Wesley, Reading, Mass.,

1961), Sec. 11-7 for a discussion of time-dependent perturbation theory.

¹³See, for instance, D. M. Brink and G. R. Satchler, *Angular Momentum*, 2nd ed. (Oxford University, London, 1975).

¹⁴A. Corney, *Atomic and Laser Spectroscopy* (Oxford University, London, 1979), Chap. 15.

¹⁵E. T. Jaynes and F. W. Cummings, *Proc. IEEE* **51**, 89 (1963).

¹⁶C. R. Stroud, Jr., *Phys. Rev. A* **3**, 1044 (1971).

¹⁷A. M. Bonch-Bruевич and V. A. Khodovoi, *Usp. Fiz. Nauk* **93**, 71 (1967) [*Sov. Phys.—Usp.* **10**, 637 (1967)].

¹⁸See Ref. 7, formula 2.

¹⁹P. F. Liao and J. E. Bjorkholm, *Phys. Rev. Lett.* **34**, 1 (1975).

²⁰A. M. Bonch-Bruевич, N. N. Kostin, V. A. Khodovoi, and V. V. Khomov, *Zh. Eksp. Teor. Fiz.* **56**, 144 (1969) [*Sov. Phys.—JETP* **29**, 82 (1969)].

²¹W. Hanle, *Z. Phys.* **30**, 93 (1924).

²²P. A. Frankin, *Phys. Rev.* **121**, 508 (1961).

²³A. Lurio, R. L. DeZafra, and R. J. Goshen, *Phys. Rev.* **134**, A1198 (1964).

²⁴A. Corney, *Atomic and Laser Spectroscopy* (Oxford University, London, 1979), Chap. 15.

²⁵M. Broyer, G. Gouedard, J. C. Lehmann, and J. Vigue, in *Advances in Atomic and Molecular Physics*, edited by D. R. Bates and B. Bederson (Academic, New York, 1976), Vol. 12.

²⁶A lucid discussion of the classical model as well as the role of coherent superposition of eigenstates in the Hanle effect has been given by R. N. Zare, *Accounts Chem. Res.* **4**, 361 (1972).